Fusing Rigid Spin Probes to Paramagnetic Sandwiches. Synthesis, Crystal Structures, and NMR Spectroscopy of Bis(isodicyclopentadienyl)metal Compounds†

Irene Gattinger, Martin A. Herker, Wolfgang Hiller, and Frank H. Köhler*

Anorganisch-chemisches Institut, Technische Universität München, D-85747 Garching, Germany

Received October 23, 1998

To probe the sign of the unpaired spin density on the ligands of metallocenes neutral and cationic derivatives which contained the isodicyclopentadienyl (Isodicp) ligand have been synthesized. The resulting compounds have the composition $(Isodicp)_2M$ [M = Fe (**3**), V (**4**), Cr (**5**), Ni (**7**)], and the corresponding salts are $(Isodicp)_2M^+PF_6^-$ ($M^+ = Fe^+$) (**3**$^+PF_6^-$), Cr^+ (**5**$^+PF_6^-$), Co^+ (**6**$^+PF_6^-$), Ni^+ (**7**$^+PF_6^-$). While the *exo*,*exo*-, *exo*,*endo*-, and *endo*,*endo*-isomers (**a**, **b**, and **c**, respectively) are conceivable, **4a**, **5a**, **5a**$^+PF_6^-$, **7**, and **7a**$^+PF_6^-$ have been isolated as the only isomers. By contrast, mixtures of **3a** and **3b**, **3a**$^+PF_6^-$ and **3b**$^+PF_6^-$, as well as **6a**$^+PF_6^-$, **6b**$^+PF_6^-$, and **6c**$^+PF_6^-$ have been obtained; **3a** and **3a**$^+PF_6^-$ could be separated by crystallization. Metal-dependent ligand exchange is proposed to be responsible for the isomer distribution. All compounds have been investigated by ^1H and ^{13}C NMR spectroscopy. The diamagnetic species **3a**, **3b**, **6a**$^+PF_6^-$, and **6b**$^+PF_6^-$ served as NMR standards for the neutral and cationic paramagnetic species, respectively. X-ray crystal structure analyses of **3a**$^+PF_6^-$ and **5a**$^+PF_6^-$ provided similar geometrical data which were used to calculate the dipolar signal shifts and subsequently the contact shifts (δ^{con}) of all paramagnetic compounds. The two different carbons which are separated from the Cp ring by two bonds (β carbons) have been used as probes for the spin sign. From the difference of their δ^{con} values negative spin could be established in the ligand π orbitals of the vanadocene, chromocene, chromocenium ion, and ferrocenium ion; for the nickelocene and nickelocenium ion the spin was positive. This method proved to be most reliable, because the perturbation by σ spin delocalization could be strongly reduced. The spin-carrying orbitals were analyzed on the basis of MO calculations.

Introduction

The focus of the present work is the design of paramagnetic sandwich compounds that allow to probe the unpaired electron spin density within the ligand sphere of open-shell π complexes in general. The interest in spin densities goes back to the fact that the magnetic properties of molecular solids often depend on (extended) interactions between lattice neighbors.[1] These interactions in turn are determined by the spin density.[2] In favorable cases, ferromagnetism occurs, and a transition to bulk magnets can be achieved.[1,2] Therefore, it is desirable to have criteria at hand that guide the rational design of new magnetic materials.

An important criterion is the sign of the magnetic moment associated with the spin density (hereafter shortened to "sign of the spin density"). When the magnetic interaction is best described by analogy to Heitler−London spin exchange as proposed by McConnell[3] the sign of the spin density must be negative and positive in the relevant areas of the interacting species, respectively. This mechanism has been suggested by Kollmar et al.[4] to explain the magnetic interaction between the decamethylmetallocenium ions $[(\eta^5\text{-}C_5Me_5)_2M]^+$ and, e.g., tetracyanoethinide ($TCNE^-$). We refer to this as the McConnell−Kollmar−Kahn (MKK) mechanism. In the crystal the two ions form stacks,[5] two repeat units of which are shown in Figure 1. Also shown (by arrows) are the relative signs of the spin density in the π orbitals of both ions, which have been postulated[4] for M = Cr, Mn, and Fe to account for the ferromagnetic interaction and the spontaneous magnetization that has been found experimentally for this type of compounds.[6] For the case M = Ni antiferromagnetic interaction has been reported,[7] and the sign of the spin density in the π system of nickelocenium has been postulated to be inverted.[4] Hence, for M = Ni all spin arrows in the neighboring planes of Figure 1 should be parallel.

Previous Approach to Spin Densities. The sign of the spin density in the π orbitals of sandwich compounds can be determined by NMR spectroscopy. In previous studies[8] we have demonstrated that this is severely hampered when the metal-

† Dedicated to Prof. Helmut Werner on the occasion of his 65th birthday.

(1) (a) Kahn, O. *Molecular Magnetism*; VCH Publishers: Weinheim, 1993. (b) Gütlich, P.; Hauser, A.; Spiering, H. *Angew. Chem., Int. Ed. Engl.* **1994**, *33*, 2024. (c) Miller, J. S.; Epstein, A. J. *Angew. Chem., Int. Ed. Engl.* **1994**, *33*, 385. (d) Veciana, J.; Cirujeda, J.; Rovira, C.; Vidal-Gancedo, J. *Adv. Mater.* **1995**, *7*, 221.
(2) Kollmar, C.; Kahn, O. *Acc. Chem. Res.* **1993**, *26*, 259.
(3) McConnell, H. M. *J. Chem. Phys.* **1963**, *39*, 1910.
(4) Kollmar, C.; Couty, M.; Kahn, O. *J. Am. Chem. Soc.* **1991**, *113*, 7994. Kollmar, C.; Kahn, O. *J. Chem. Phys.* **1992**, *96*, 2988.
(5) Miller, J. S.; Calabrese, J. C.; Epstein, A. J.; Bigelow, R. W.; Zang, J. H.; Reiff, W. M. *J. Chem. Soc., Chem. Commun.* **1986**, 1026.
(6) (a) Miller, J. S.; Calabrese, J. C.; Rommelmann, H.; Chittapeddi, S. R.; Zang, J. H.; Reiff, W. M.; Epstein, A. J. *J. Am. Chem. Soc.* **1987**, *109*, 769. (b) Chittapeddi, S.; Cromack, K. R.; Miller, S. J.; Epstein, A. J. *Phys. Rev. Lett.* **1987**, *58*, 2695. (c) Miller, J. S.; O'Hare, D. M.; Chakraborty, A.; Epstein, A. J. *J. Am. Chem. Soc.* **1989**, *111*, 7853. (d) Broderick, W. E.; Thompson, J. A.; Day, E. P.; Hoffmann, B. M. *Science* **1990**, *249*, 401. (e) Yee, G. T.; Manriques, J. M.; Dixon, D. A.; McLean, R. S.; Groski, D. M.; Flippen, R. B.; Narayan, K. S.; Epstein, A. J.; Miller, J. S. *Adv. Mater.* **1991**, *3*, 309. (f) Broderick, W. E.; Hoffman, B. M. *J. Am. Chem. Soc.* **1991**, *113*, 6334. (g) Broderick, W. E.; Eichhorn, D. M.; Liu, X.; Toscano, P. J.; Owens, S. M.; Hoffman, B. M. *J. Am. Chem. Soc.* **1995**, *117*, 3641.
(7) Miller, J. S.; Epstein, A. J.; Reiff, W. M. *Chem. Rev.* **1988**, *88*, 201.
(8) (a) Blümel, J.; Hebendanz, N.; Hudeczek, P.; Köhler, F. H.; Strauss, W. *J. Am. Chem. Soc.* **1992**, *114*, 4223. (b) Blümel, J.; Hebendanz N.; Hudeczek, P.; Köhler, F. H.; Steck, A.; Strauss, W. *Mol. Cryst. Liq. Cryst.* **1993**, *233*, 153.

10.1021/ic9812407 CCC: $18.00
Published on Web 04/21/1999

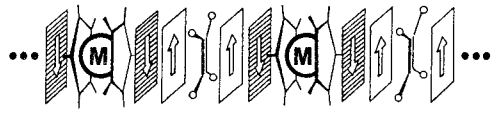

Figure 1. Two repeat units of a $[(C_5Me_5)_2M]^+[TCNE]^-$ stack. Open circles represent CN substituents, the planes represent the π clouds at the periphery of the metallocenium ions (shaded) and of $TCNE^-$ (nonshaded), and the arrows represent the spin engaged in the magnetic exchange.

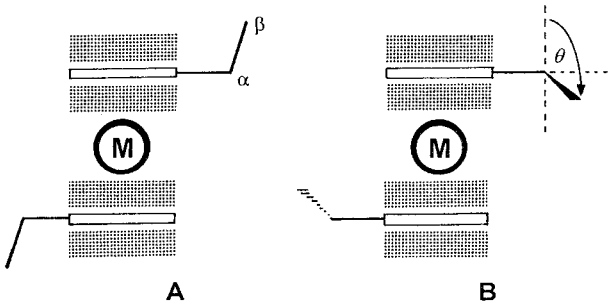

Figure 2. Side view of sandwich compounds. The substituents dispose of carbon atoms in β positions, and in **A** and **B** they are oriented differently relative to the (shaded) ligand π systems.

to-ligand spin transfer is effected not only by π but also by σ delocalization. An important example is $[(\eta^5\text{-}C_5Me_5)_2Fe]^+$, whose $[TCNE]^-$ derivative is the prototype of the magnetic materials in question.[6a]

The NMR detection of the spin density becomes more reliable when it can be made π-selective by exploiting hyperconjugation as a "filter". Thus in principle, and as shown in Figure 2, sandwich compounds **A** and **B** were studied whose substituents had different dihedral angles θ between the ligand π system and the Cα−Cβ bond. For consequence, the β-carbon atoms sensed the π spin more (**A**) or less (**B**) efficiently following the relation[9]

$$\delta^{con}(^{13}C) = \delta_o(^{13}C) + B(^{13}C)\cos^2\theta \qquad (1)$$

Here the (Fermi) contact shift δ^{con} is composed of a hyperconjugational term $B\cos^2\theta$ (with B being a constant) and of a term δ_o which accounts for all other shift contributions.

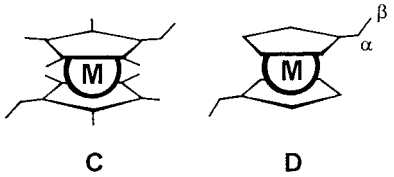

Experimentally, cases **A** and **B** of Figure 2 were realized by the ethyl-substituted metallocenes **C** and **D**.[8] In **C** an angle $\theta = 0°$ was forced by neighboring methyl groups while the average angle $\theta = 45°$ resulted for the sum of the methyl rotamers of **D**. As a result, the β-carbon signal should move to high frequency when passing from **C** to **D** and when the π spin density is negative. As for the ferromagnetic interaction in $[(C_5Me_5)_2M]^+[TCNE]^-$, no exception from the MKK mechanism was found when the π spin densities of the metallocenium ions were checked following these lines. More precisely, the π spin density is negative for M = Cr, Mn, and Fe (and for M = Cr, Mn in the neutral congeners), while it is positive for M = Ni (and for the neutral cobaltocenes and nickelocenes). It should be noted that these findings did not rule out an alternative mechanism of ferromagnetic interaction which was proposed by Miller and Epstein.[10]

New Approach to Spin Densities. A limitation of the approach outlined so far is that the constants in eq 1 are specific only for a given molecule. Hence, errors may arise when the π spin is probed via the different dihedral angles θ of *two* sandwiches. As described in more detail previously,[8a] the reason is that, for instance, the metal-to-ligand spin transfer may vary, and the different substitution patterns (as in **C** and **D**) will also introduce some scatter. The worst case would be that these effects overcompensate the aforementioned π spin-driven shift of the β-carbon signal which is observed for the sandwiches **C** and **D**. Actually, we had overlooked the pair $(EtMe_4C_5)_2V$ ($\delta(C\beta) = 540$[11a]) and $(EtC_5H_4)_2V$ ($\delta(C\beta) = 420$[11b]). Here the shift change is just opposite to what is expected for negative π spin that was claimed for vanadocenes.[11]

The approach could be improved a lot if different β-carbon atoms were present in *one* sandwich molecule. A suitable ligand is the isodicyclopentadienyl anion,[12] from which the metallocene **E** in Figure 3 is derived. A side view of the upper ligand along

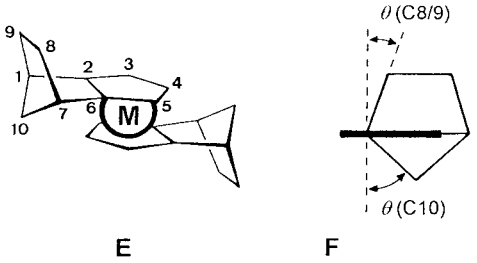

Figure 3. Bis(isodicyclopentadienyl)metal compounds (**E**); for isomers see Scheme 1. **F** shows a side view of the upper ligand of **E** along the vector C1−C2. The Cp plane is represented as a black bar. The dihedral angles important for the π spin transfer to carbons 8−10 are θ(C8/9) and θ(C10).

C1−C2 (Figure 3, **F**) visualizes the different dihedral angles θ(C8/9) and θ(C10) between the p_z orbitals at C2 and the bonds C2−C9 and C2−C10, respectively. Another advantage is the easy distinction of the β-carbon atoms which follows from the NMR signal intensities. Therefore, we have synthesized a number of bis(isodicyclopentadienyl)metal (abbreviated as $(Isodicp)_2M$) derivatives, determined the structure of representative examples, and analyzed the NMR spectra with emphasis on probing the spin densities in these compounds.

Results

Syntheses. Isodicyclopentadiene (compound **1** in Scheme 1) was synthesized by modifying literature procedures.[13] Its deprotonation afforded the anion **2** which was converted to the corresponding metallocenes **3**−**7** by reaction with the appropriate solvated metal dihalide (Scheme 1). When the metal was vanadium, chromium, and nickel, only one of the three possible isomers (Scheme 1) was found. The *exo*,*endo*-isomer (**b**) could

(9) Adapted from Heller, C.; McConnell, H. M. *J. Chem. Phys.* **1960**, *32*, 1535.

(10) Miller, J. S.; Epstein, A. J. *J. Am. Chem. Soc.* **1987**, *109*, 3850.

(11) (a) Köhler, F. H.; Doll, K. H.; Prössdorf, W. *J. Organomet. Chem.* **1982**, *224*, 341. (b) Köhler, F. H. *J. Organomet. Chem.* **1976**, *110*, 235. Note that the sign convention has been changed since.

(12) Riemschneider R.; Heymons, K. *Monatsh. Chem.* **1961**, *92*, 1080. Riemschneider R. *Z. Naturforsch. B* **1962**, *17*, 133.

(13) (a) Alder, K.; Stein, G. *Ber. Dtsch. Chem. Ges.* **1934**, *67*, 613. Alder, K.; Stein, G. *Liebigs Ann. Chem.* **1931**, *485*, 211; **1933**, *501*, 1. (b) Rosenblum, M. *J. Am. Chem. Soc.* **1957**, *79*, 3179. Mironov, V. A.; Lukýanov, V. T. Bernadskii, A. A. *J. Org. Chem. USSR, Engl. Transl.* **1984**, *20*, 61.

Scheme 1 [a]

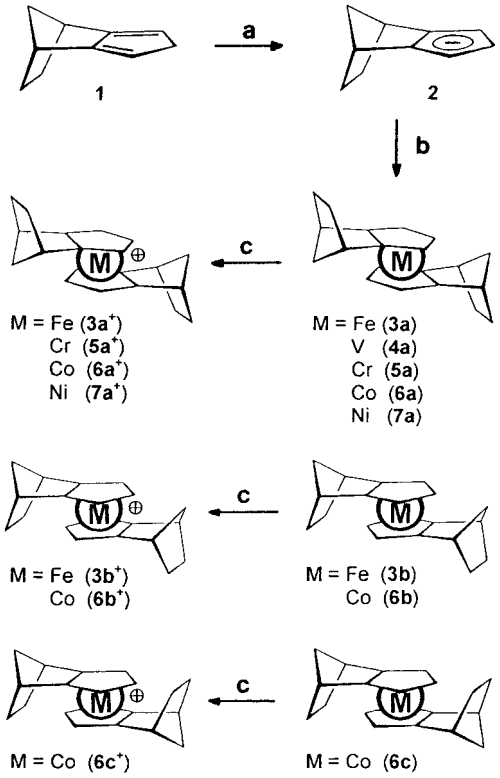

[a] Key: (a) *n*-BuLi; (b) $MX_2(THF)_n$; (c) $Ag^+PF_6^-(MeCN)_3$ or $Cp_2Fe^+PF_6^-$ or $FeCl_3$; a = *exo,exo-*, b = *exo,endo-*, and c = *endo,endo-*isomer.

be excluded, because only one set of ligand resonances was present in the NMR spectra. The *exo,exo*-isomer (**a**) was established for chromium (**5a**) by oxidation and X-ray crystallography of $\mathbf{5a}^+PF_6^-$ (see below) and for nickel (**7a**) by a previous X-ray study.[14] For vanadium the *exo,exo*-isomer **4a** was assumed, because whenever more than one isomer was obtained, the *endo,endo*-isomer (**c**) was by far the least abundant.

For iron and cobalt up to three isomers were found. This corresponds to previous work on ferrocenes,[15] which were reinvestigated as precursors of the desired ferrocenium salts and as diamagnetic reference compounds for the NMR studies of the neutral paramagnetic congeners. According to NMR spectroscopy the isomers **3a** and **3b** were obtained in ratios between $^1/_4$ and $^1/_9$ when the reaction was carried out at 40 °C and in a ratio of 1/12 at −78 °C. Efforts to separate **3a** and **3b** by medium-pressure liquid chromatography (MPLC) failed, but fractional crystallization from acetone[15d] gave pure (^{1}H NMR) **3a** and a sample of **3b** which contained less than 20% of **3a**. The cobaltocene isomers could not be separated either as neutral compounds or via the cations (see below). In a sample of the neutral cobaltocenes the *exo,exo*- and the *exo,endo*-isomers **6a** and **6b** were found in a ratio of 1/3.5 by ^{1}H NMR spectroscopy (signal shifts relative to the corresponding signals of **3a** and **3b**: **6a**, δ, −91.9 (H3/5), −28.1 (H4); **6b**, *exo*- and *endo*-coordinated ligand, respectively, δ, −76.8 and −69.3 (H3/5), −21.3 and −18.0 (H4)).

(14) Scroggins, W. T.; Rettig, M. F.; Wing, R. M. *Inorg. Chem.* **1976**, *15*, 1381.

(15) (a) Katz, T. J.; Mrowca, J. J. *J. Am. Chem. Soc.* **1967**, *89*, 1105. (b) Köhler, F. H.; Matsubayashi, G. *J. Organomet. Chem.* **1975**, *96*, 391. (c) Hsu, L. Y.; Hathaway, S. J.; Paquette, L. A. *Tetrahedron Lett.* **1984**, *25*, 259. (d) Paquette, L. A.; Schirch, P. F. T.; Hathaway, S. J.; Hsu, L. Y.; Galluci, J. C. *Organometallics* **1986**, *5*, 490. (e) Bhide, V.; Rinaldi, P.; Farona, M. F. *J. Organomet. Chem.* **1989**, *376*, 91.

Table 1. Selected Structural Parameters of Bis(isodicyclopentadienyl)metal Compounds

	compound		
distances and angles[a]	$\mathbf{3a}^+PF_6^-$	$\mathbf{5a}^+PF_6^-$	**7a**[b]
M−Cp [Å]	1.72	1.85	1.82
interligand twist angle	24.7°	23.8°	111.9°
Cp interplanar angle	3.8°	1.4°	0.2°
α	9.1°	9.7°	6.9°
ϑ(C8/9)	109.3°	109 7°	111.6°
ϑ(10)	127.8°	127.8°	127.5°
θ(C8/9)	19.3°	19.3°	19.9°
θ(10)	57.3°	57.5°	57.3°

[a] See definition of angles in Figures 3 (**F**) and 4 (**G**). Mean values of two ligands. [b] Calculated from the structure data given in ref 14.

Oxidation of the pure neutral isomers **3a**, **5a**, and **7a** as shown in Scheme 1 gave the cations $\mathbf{3a}^+$, $\mathbf{5a}^+$, and $\mathbf{7a}^+$ as PF_6^- salts. A sample of **3b** and **3a** in a ratio of 6/1 yielded $\mathbf{3b}^+PF_6^-$ accompanied by $\mathbf{3a}^+PF_6^-$ in the same ratio when the reaction was carried out at −78°C. At room temperature the ratio decreased, and when starting with pure **3a** some $\mathbf{3b}^+$ was found along with $\mathbf{3a}^+$. The cobaltocenium ions $\mathbf{6a}^+$, $\mathbf{6b}^+$, and $\mathbf{6c}^+$ were obtained in the ratio 2.5/4.2/1 (^{1}H NMR) from **2** and $CoCl_2$ slightly above room temperature without isolating the cobaltocenes. We were unable to separate the isomers by MPLC or fractional crystallization. Fortunately, the NMR reference data that were needed for the paramagnetic cations $\mathbf{3a}^+$, $\mathbf{3b}^+$, $\mathbf{5a}^+$, and $\mathbf{7a}^+$ could be obtained from the mixture.

All paramagnetic neutral and cationic metallocenes were air-sensitive. Solid $\mathbf{3a}^+$ and $\mathbf{3b}^+$ did not decompose when opposed to air for short periods. Yet they were routinely handled under inert gas. While the neutral sandwiches were soluble in hexane, benzene, and ethers, more polar solvents such as acetone and acetonitrile were suitable for the cations.

Crystal Structures of $\mathbf{3a}^+PF_6^-$ and $\mathbf{5a}^+PF_6^-$. For the NMR analysis the geometrical details of the isodicyclopentadienyl ligand and its coordination to transition metals were needed. Since the structure of **7a** was known[14] and since we were most interested in the structural changes that would occur upon changing the metal ion or the charge, the iron and chromium salts $\mathbf{3a}^+PF_6^-$ and $\mathbf{5a}^+PF_6^-$ were chosen as representative examples.

Both compounds crystallize in the trigonal space group $P3_121$ with the cell volume of $\mathbf{5a}^+PF_6^-$ being 3.7% larger than that of $\mathbf{3a}^+PF_6^-$. The difference is caused mainly by the different metal-Cp distances (Table 1) while the distances between the anions and cations remain almost the same. This follows from the distances of the metal from phosphorus (Fe···P = 6.332(8) Å and Cr···P = 6.313(8) Å) and from the nearest fluorine (Fe···F4 = 4.767(3) Å and Cr···F4 = 4.757(5) Å). As shown in Figure 4 the cations have idealized C_2 symmetry, and the two ligands deviate considerably from a trans arrangement with twist angles close to 24° (Table 1). A still larger angle has been found for **7a**.[14] Table 1 further documents some structural features that are important for the NMR analysis. Thus, C1 and C7 are bent away from the metal (cf. the angle α in Figure 4, **G**), the interplanar angles ϑ(C8/9) and ϑ(C10) deviate from 120°, and the dihedral angles θ(C8/9) (Figure 3, **F**) are considerably smaller than θ(C10). Similar features can be extracted from previous X-ray crystal data of other compounds containing the Isodicp ligand.[15c,16]

In conclusion, all corresponding data of the salts $\mathbf{3a}^+PF_6^-$ and $\mathbf{5a}^+PF_6^-$ are very similar except for the M−Cp distances and the Cp interplanar angles. When passing from a cationic to

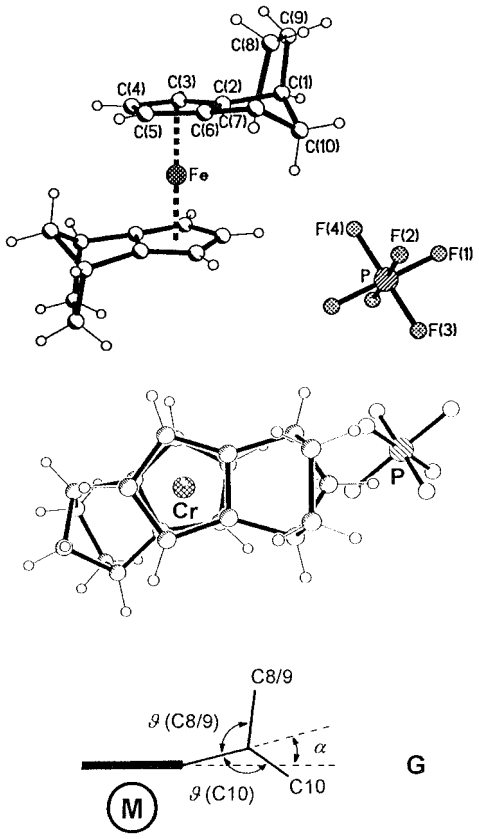

Figure 4. Molecular structures of (top) $\mathbf{3a}^{+}PF_6^{-}$ and (middle) $\mathbf{5a}^{+}PF_6^{-}$. The H atoms were calculated for idealized C−H bonds. **G** shows the definition of interplanar angles.

the neutral species there is an additional change of the angles α and ϑ(C8/9).

NMR and EPR Spectroscopies. First the ferrocenes **3a** and **3b** and the cobaltocenium ion $\mathbf{6a}^{+}$ were studied, because they were needed as diamagnetic standards for the paramagnetic neutral and cationic analogues, respectively. Bhide et al.[15e] have reported a detailed ^{1}H NMR investigation of **3**. However, unexpected signal shift differences of analogously bound ligands led us to reinvestigate **3a** and **3b**. While the data of **3a** could be perfectly reproduced, our spectra, including a 600 MHz HMQC experiment, gave rather different data for **3b** (Experimental Section and Supporting Information).

The ^{1}H and ^{13}C NMR data of $\mathbf{6a}^{+}$, $\mathbf{6b}^{+}$, and $\mathbf{6c}^{+}$ were determined from mixtures of isomers. The high-field 2D spectra were similar to those obtained for **3a** and **3b**. Quite expectedly, the Cp signals of $\mathbf{6a}^{+}$ and $\mathbf{6b}^{+}$ were shifted considerably more to high frequencies than those of **3a** and **3b**. The signal shifts of the bicyclic substituent showed some scatter caused by the change of the metal and by *exo*- or *endo*-bonding of the ligand (Experimental Section and Supporting Information).

The paramagnetic neutral compounds were reinvestigated in order to have a broad basis for the NMR studies of the new cationic compounds. It turned out that our previous results[11b] partly suffered from the low sensitivity of the spectrometers and unreliable temperature calibrations, so that revision was necessary.

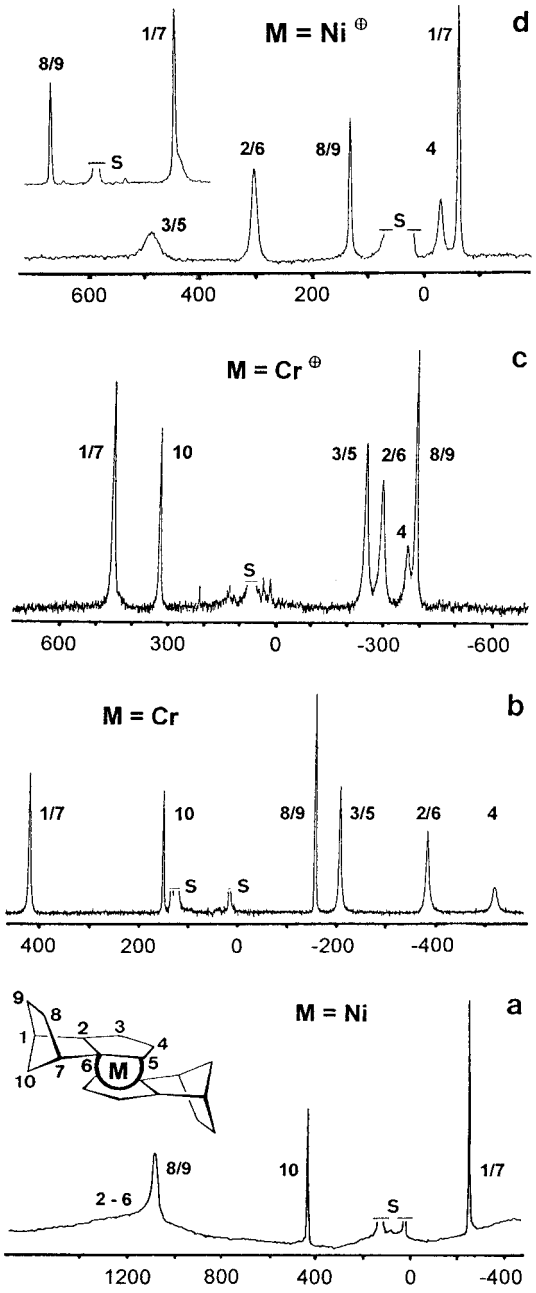

Figure 5. ^{13}C NMR spectra of (a) **7a** in toluene at 379 K, (b) **5a** in toluene at 305 K, (c) $\mathbf{5a}^{+}PF_6^{-}$ in CD_3CN at 335 K, and (d) $\mathbf{7a}^{+}PF_6^{-}$ in CD_3NO_2 at 360 K (inset at 305 K). S = solvent; scales in ppm. See text for further details.

^{13}C NMR spectroscopy gave the most simple spectra which consisted of six signals for a pure *exo*,*exo*-isomer. Their assignment is illustrated by representative spectra reproduced in Figure 5. For the nickel derivative **7a** the three expected Cp signal appear as a very broad, unresolved feature between roughly 1000 and 1400 ppm (Figure 5a). This is in accord with previous results[17] when the temperature dependence of the signal shifts is considered. The signal near −250 ppm is typical[17] for

(16) (a) Paquette, L. S.; Hathaway, S. J.; Schirch, P. F. T.; Gallucci, J. C. *Organometallics* **1986**, *5*, 500. (b) Gallucci, J. C.; Gautheron, B.; Gugelchuk, M.; Meunier, P.; Paquette, L. A. *Organometallics* **1987**, *6*, 15. (c) Paquette, L. A.; Moriarty, K. J.; Meunier, P.; Gautheron, B.; Sornay, C.; Rogers, R. D.; Rheingold, A. L. *Organometallics* **1989**, *8*, 2159. (d) Zaegel, F.; Gallucci, J. C.; Meunier, P.; Gautheron, B.; Sivik, M. R.; Paquette, L. A. *J. Am. Chem. Soc.* **1994**, *116*, 6466. (e) Herberich, G. E.; Jansen, U. J. *Organometallics* **1995**, *14*, 834. (f) Gallucci, J. C.; Gobley, O.; Zaegel, F.; Meunier, P.; Gautheron, B.; Lange, H.; Gleiter, R.; Kozmina, N.; Paquette, L. A. *Organometallics* **1998**, *17*, 111.

(17) Köhler, F. H.; Doll, K.-H.; Prössdorf, W. *Angew. Chem., Int. Ed. Engl.* **1980**, *19*, 479.

carbons next to Cp, and therefore it is assigned to C1/7. The remaining signals have an area ratio of about 2/1, and hence the less-shifted one belongs to C10 and the more-shifted one to C8/9; details are collected in Table 2.

For the chromium derivative **5a** (Figure 5b) the Cp carbons are expected to give rise to a 2/2/1 pattern at low frequency while a high-frequency signal should appear for C1/7.[11a,18] The only other signal of relative intensity 1 must belong to C10 and is found near 150 ppm. The signal of C8/9 was identified by a partly resolved ^1J(CH) triplet. Generally, no ^1J(CH) couplings were observed for the Cp signals, because the relaxation of the corresponding ^{13}C and ^{1}H nuclei was too fast. These signals were distinguished by considering the spin density distribution on the five-membered ring, which leaves only two choices for the signal sequence:[18] $|\delta(C4)| > |\delta(C2/6)| > |\delta(C3/5)|$ or vice versa. It follows that for **5a** the signals close to −200 and −380 ppm belong to C3/5 and C2/6, respectively.

Next we turn to the cationic chromium derivative **5a**$^+$. Its ^{13}C NMR spectrum (Figure 5c) is similar to that of **5a**, and again the signals of C2−6 and C1/7 appear in the known ranges.[8] However, it was not immediately clear which of the low-frequency signals belonged to C8/9, because the signal half-widths (W) did not allow us to reliably identify a ^1J(CH) triplet. Instead the assignment was derived from the fact that W is determined by dipolar and contact relaxation.[11] If the latter dominates W increases with δ^2. Obviously, this does not hold for **5a**$^+$, because the signal near −390 ppm is narrower than those near −300 and −250 ppm. It follows that the dipolar relaxation must be most important, and in this case $W \propto r^{-6}$ applies (r is the distance between the metal and the ^{13}C or ^{1}H nucleus under study). In fact, r(Cr−C8/9) is twice as large as r(Cr−C2,3,4,5,6) so that the narrow signal near −390 ppm must belong to C8/9 while the broad ones near −250 and −300 are those of C3/5 and C2/6, respectively.

The ^{13}C NMR spectrum of the *exo,exo* ferrocenium derivative **3a**$^+$ could be assigned unambiguously by using the methods already mentioned. In particular, C10 and C8/9 were identified by the ^1J(CH) triplet structures of the signals near −55 and −90 ppm, thus establishing an unusually small signal shift difference for these nuclei. In the case of **3b**$^+$ each of the exo- and endo-bound ligands gave one set of signals. For the assignment it seemed reasonable to assume that all signals shifts of the exo-bound ligand appeared closer to those of the *exo,exo*-isomer **3a**$^+$ than those of the endo-bound ligand.

The ^{13}C NMR spectrum of the nickelocenium derivative **7a**$^+$ at 305 K (Figure 5d) showed only four signals of equal intensity. Comparison with the known signal shift ranges[8] and consideration of W led to the assignment given in Figure 5d and Table 2. The signal near −80 ppm had a shoulder at low frequency (inset of Figure 5d) which could be due to C4 or C10. When the temperature was increased a well-separated signal was detected that moved to high frequency more rapidly than that of C1/7. If the new signal belonged to C10 its width should be similar to that of C1/7, and a triplet structure should be visible. However, W was much greater (Table 2) so that the new signal had to be assigned to C4. C10 was suspected to be hidden under the solvent signal, but it could not be detected by increasing the temperature and by changing the solvent. In either case decomposition occurred. Eventually, C10 was established by solid-state MAS NMR spectroscopy.

In the ^{1}H NMR spectra the isodicyclopentadienyl ligand shows 11 signals. While the Cp protons are easy to assign owing to the large signal shifts and/or widths, it is more difficult to identify the protons of the substituent, because the signal shift differences are sometimes small. Scroggins et al.[14] have convincingly assigned the ^{1}H NMR spectrum of **7** by selctive deuteriation and confirmed that the interaction between spin in a π orbital and γ protons is most efficient when the intermediate bonds adopt a W arrangement as illustrated in Figure 6. The W concept, which has been studied in detail,[20] implies that for the isodicyclopentadienyl ligand the signals of the *anti*-protons should be more shifted than those of the corresponding *syn*-protons. The sign of these shifts should be the same as that of the spin in the Cp π orbitals.

While the W concept is useful for assigning the ^{1}H NMR signals of **7a**$^+$ (Table 2), difficulties arise when dipolar signal shifts and more complicated electron spin delocalization interfere. An example is the ^{1}H NMR spectrum of the ferrocenium ion **3a**$^+$ in Figure 7. The signal assignment is greatly facilitated by the fact that the dipolar relaxation dominates the signal half-widths W. Thus H3−5 which are closest to Fe have the broadest signals, and the signal of H1/7 is broader (although less shifted) than that of H10-*anti* which in turn is much smaller than that of H10-*syn*. The assignment of H10-*syn*/*anti* given in the top of Figure 7 is opposite to that expected from the W concept. This is an example where the W concept is overruled by the difference of the dipolar shifts (see below). Following these lines the ^{1}H NMR spectrum of the *exo,endo*-isomer **3b**$^+$ (Figure 7) could be assigned except for the broad feature of H3−5 that was disturbed by other signals.

The ^{1}H NMR spectrum of **5a** is qualitatively rather similar to that of **3a**$^+$ while those of **4a** and **5a**$^+$ are different (Supporting Information). Because of strong signal overlap three signals of **4a** were assigned tentatively (Table 2). The other signal assignments of **4a** and **5a**$^+$ are based on the shift ranges, integrals, and signal half-widths.

The EPR spectrum of solid **3a**$^+$PF$_6^-$ diluted in **6**$^+$PF$_6^-$ showed features attributable to $g_{\|} = 3.9561$ and $g_{\perp} = 2.0560$. This is characteristic for the $^2E_{2g}$ ground state of ferrocenium ions[21] although the g factor anisotropy is smaller than in many other cases. The solid-solution EPR spectrum of **5a**$^+$PF$_6^-$ in acetone was analyzed as previously done for Cp$_2$Cr$^+$ [22] which has a $^4A_{2g}$ ground state; the result was $g_{\|} = 1.911$ and $g_{\perp} = 1.7985$.

Discussion

Cp π-Face Isomers. Ample preparative, structural, NMR, and computational evidence has been collected by Paquette, Gautheron, Gleiter, Bauer, and associates (see recent literature compilation in refs 16e and f) which demonstrates that at ambient temperature the isodicyclopentadienyl anion (**2**) is

(18) (a) Köhler, F. H.; Doll, K.-H. *Z. Naturforsch. B* **1982**, *37*, 144. (b) Köhler, F. H.; Geike, W. A. *J. Organomet. Chem.* **1987**, *328*, 35. (c) Blümel, J.; Hofmann, P.; Köhler, F. H. *Magn. Reson. Chem.* **1993**, *31*, 2.

(19) (a) Kowalewski, J.; Nordenskiöld, L.; Benetis, N.; Westlund, P. O. *Prog. Nucl. Magn. Reson. Spectrosc.* **1985**, *17*, 141. (b) Bertini, I.; Lucinat, C. *NMR of Paramagnetic Molecules in Biological Systems*; The Benjamin/Cummings Publishing Company: Menlo Park, CA, 1986; Chapter 3. (c) Banci, L.; Bertini, I.; Luchinat, C. *Nuclear and Electron Relaxation*; VCH Publishers: Weinheim, 1991; Chapter 7.

(20) (a) Russell, G. A.; Chang, K.-Y. *J. Am. Chem. Soc.* **1965**, *87*, 4381. (b) Russel, G. A.; Chang, K.-Y.; Jefford, C. W. *J. Am. Chem. Soc.* **1965**, *87*, 4383.

(21) (a) Prins, R. *Mol. Phys.* **1970**, *19*, 603. (b) Prins, R.; Korswagen, A. R.; Kortbeck, A. G. T. G. *J. Organomet. Chem.* **1972**, *39*, 335. (c) Horsfield, A.; Wassermann, A. *J. Chem. Soc., Dalton Trans.* **1972**, 187. (d) Duggan, D. M.; Hendrickson, D. N. *Inorg. Chem.* **1975**, *14*, 955.

(22) Ammeter, J. H. *J. Magn. Reson.* **1978**, *30*, 299.

Table 2. ^{1}H and ^{13}C NMR Data[a] of Neutral and Cationic Bis(isodicyclopentadienyl)metal Compounds

	compounds and signal shifts(widths)															
					3b^{+}											
nucleus	**4a**		**3a**$^{+}$		*exo*-ligand		*endo*-ligand		**5a**		**5a**$^{+}$		**7a**		**7a**$^{+}$	
and position[b]	δ^{exp} [c] (W)	δ^{con}	δ^{exp} (*W*)	δ^{con}	δ^{exp} (*W*)	δ^{con}	δ^{exp} (*W*)	δ^{con}	δ^{exp} (*W*)	δ^{con}	$\delta^{exp,g}$ (*W*)	δ^{con}	$\delta^{exp,h}$ (*W*)	δ^{con}	δ^{exp} (*W*)	δ^{con}
H3/5	235 (3630)	279	28.1 (800)	16.3	27−30 [d]	15−17 [d]	27−30 [d]	15−17 [d]	298 (2180)	312	340 (5200)	330	−261 (1210)	−261	−174 (3580)	−183
H4	235 (3630)	278	29.7 (1200)	15.6	27−30 [d]	15−17 [d]	27−30 [d]	15−17 [d]	403 (3300)	419	510 (5300)	501	−280 (1440)	−281	−30.8 (230)	−36.5
H1/7	1.0 [d] (*d*)	−0.8	−11.5 (110)	−13.1	−9.0 (115)	−10.1	−11.3 (60)	−12.3	−6.6 (190)	−14.6	−2.8 (495)	−4.3	28.8 (100)	24.0	6.4 (75)	2.7
H8/9-*syn*	27.7 (122)	29.3	24.6 (75)	−0.5	28.1 (50)	3.2	−40.2 (265)	33.4	11.5 (100)	20.5	3.9 (90)	−1.5	0.7 (150)	3.4	3.4 (65)	3.5
H8/9-*anti*	3.1 [d] (*d*)	0.6	8.6 (30)	0.9	7.0 (45)	−0.4	21.2 (70)	41.6	4.1 (40)	5.6	8.4 (135)	5.1	102.5 (110)	102.0	45.2 (280)	44.6
H10-*syn*	10.4 (130)	20.5	−61.6 (280)	12.6	−48.4 (325)	26.1	25.5 (105)	−2.4	−16.1 (645)	−48.6	53.8 (1950)	62.0	−1.0 (280)	−14.6	1.0 (130)	−4.3
H10-*anti*	1.0 [d] (*d*)	2.7	−15.7 (55)	−4.7	−24.1 (55)	−12.7	7.3 (115)	5.6	−9.8 (90)	−18.1	12.8 (240)	13.3	24.9 (50)	21.0	1.9 (65)	−0.5
C2/6	−434 (1700)	−644	199.6 (205)	−110.4	183.4 (185)	−108.4	131.5 (194)	−170.5	−381.0 (525)	−389.1	−299.6 (945)	−459	1150[i]	*k*	355 (945)	255
C3/5	−548 (2180)	−736	307.6 (205)	19.9	283.6 (165)	15.3	269.1 (215)	3.0	−203.5 (330)	−176.0	−254 (720)	−371	1150[i]	*k*	552 (2580)	498
C4	−417 (850)	−595	−139.5 (215)	−180.1	95.5 (215)	−201.7	74.2 (240)	−219.3	−518 (740)	−502	−369 (860)	−499	1150[i]	*k*	−78.5 (340[m])	−155
C1/7	554 (1380)	597	26.9 [f] (180)	−12.4	53.2 [f] (120)	16.1	62.2 [f] (180)	25.2	422.2 (305)	390.5	452 (540)	422	329[j] (280)	−366	−78.5 [f] (150[m])	−118.1
C8/9	−38.8 [e] (230)	−80.7	−88.8 [e] (180)	−136.0	−94.1 [e] (110)	−143.0	−160 (140)	−148.0	−153.4 [e] (150)	−194.1	−392 (485)	−432	1401[j] (1560)	1376	143.7 [e] (180[m])	118.8
C10	617 (1130)	663	−55.7 [e] (180)	24.8	−33.5 (275)	49.6	27.1 (280)	12.9	153.5 (240)	95.6	322 (335)	274	556[j] (330)	503	67.8 [n] (900)	19.1

[a] Signal shifts in ppm; δ^{exp} at 305 K (unless stated otherwise) relative to TMS; δ^{con} contact shift (see text) at 298 K; *W* signal width at half-height in Hz. [b] Numbering see Figures 5 and 7. [c] ^{1}H NMR at 365 K, ^{13}C NMR at 345 K. [d] Broad feature. [e] ^{1}J(C,H) triplet resolved. [f] ^{1}J(C,H) doublet resolved. [g] ^{1}H NMR at 297 K. [h] ^{1}H NMR at 298 K. [i] Very broad unresolved feature at 379 K. [j] At 298 K. [k] Conversion of δ^{exp} to δ^{con} not meaningful (see text). [l] Shoulder of the signal of C1/7. [m] At 360 K. [n] MAS NMR at 316 K.

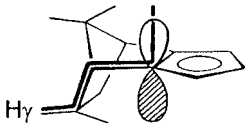

Figure 6. Preferred path of spin delocalization from a Cp π orbital to protons that are three bond away (γ protons). A corresponding path can be drawn for Hγ of the methylene bridge.

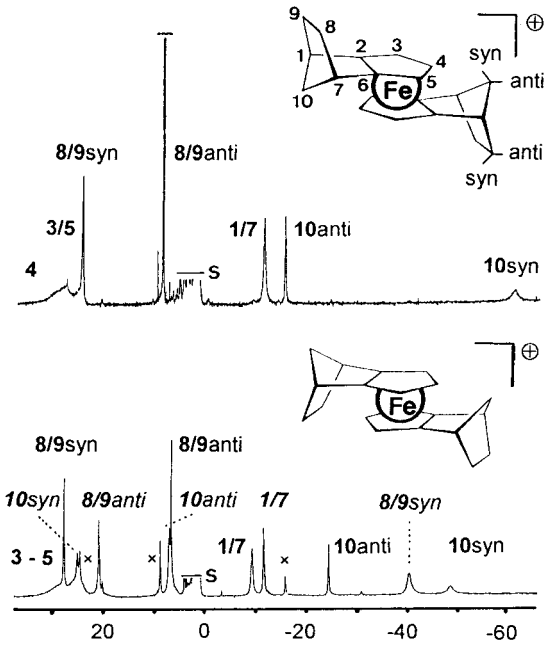

Figure 7. ^{1}H NMR spectra of (bottom) $\mathbf{3a}^+PF_6^-$ and (top) $\mathbf{3b}^+PF_6^-$ in acetone-d_6 at 305 K. Assignment of *exo*- and *endo*-ligands in normal letters and italics, respectively. S = solvent, x = signals of $\mathbf{3a}^+PF_6^-$. The scale (in ppm) refers to both spectra.

attacked by electrophiles preferably at the face next to the methano bridge (*exo*-face). Therefore, it is not surprising that the *exo*,*exo*-isomer was obtained for all sandwich compounds of this work and that it was the predominating isomer when the *exo*,*endo*- and *endo*,*endo*-isomers were formed as well. It did surprise us, however, that the isomer ratio was strongly dependent on the metal. When **2** was allowed to react with $MX_2(THF)_n$ at 40 °C, the *exo*,*exo*-isomer was found exclusively for M = V, Cr, and Ni, whereas additional isomers appeared when M was Fe and Co.

An obvious reason derives from the rearrangement that was observed for the *exo*,*endo*-ferrocenium ion $\mathbf{3b}^+$. While the starting ferrocene $\mathbf{3b}^+$ contained about 17% of **3a**, the content of $\mathbf{3a}^+$ in $\mathbf{3b}^+$ after oxidation had increased to 23% (^{1}H NMR) and some days later to 29% (^{13}C NMR). This means that the thermodynamically more stable *exo*,*exo*-isomer was formed via ligand exchange. Herberich et al.[16e] have established an equilibrium between *endo*- and *exo*-(Isodicp)Ru(C_5Me_5), where the *exo*-isomer is more stable and the reaction is catalyzed by $[(C_5Me_5)Rh(acetone)_3]^{2+}$.

Manipulation of the barrier to isodicyclopentadienyl exchange will not only be possible by a catalyst but also by changing the metal. In fact, the propensity of Cp_2M to undergo Cp exchange increases in the order Fe,Co $\ll$ V $<$ Ni $\ll$ Cr.[23] Therefore, we assume that in our reactions all isomers of $(Isodicp)_2M$ are formed. When M is V, Cr, and Ni rapid isomerization occurs, and only the most stable *exo*,*exo*-isomer is found. When M is Fe and Co the isomerization is much slower so that the *exo*,*endo*- and partly the *endo*,*endo*-isomer survive.

Probing the Sign of the Spin Density. As mentioned in the Introduction the spin density is related to the contact shift (δ^{con}). The δ^{con} values were obtained by subtracting first the shifts δ^{dia} that the molecule had if it were diamagnetic and subsequently the dipolar shifts (δ^{dip}). For the neutral and cationic compounds δ^{dia} was obtained from the ferrocene **3a** and the cobaltocenium ions $\mathbf{6a}^+$ and $\mathbf{6b}^+$, respectively (Experimental Section), and δ^{dip} was calculated as described previously[24] (Supporting Information). The resulting δ^{con} values are compiled in Table 2.

The key resonances for probing the spin density are those of C8/9 and C10. As for the dependence of δ^{con}(C8/9) and δ^{con}(C10) on the dihedral angles θ, which is given in eq 1, the discussion applies for all $(Isodicp)_2M$ derivatives, because the geometry of the ligand hardly changes with M (Table 1). With the mean dihedral angles of $\mathbf{3a}^+$ and $\mathbf{5a}^+$ θ(C8/9) = 19.3° and θ(C10) = 54.7° we obtain

$$\delta^{con}(C8/9) = \delta_o(C8/9) + 0.89B \quad (1a)$$

$$\delta^{con}(C10) = \delta_o(10) + 0.29B \quad (1b)$$

The second term represents the selective (hyperconjugative) spin transfer from the Cp π orbitals to C8/9 and C10, respectively. The sign of the constant B is the same as that of the spin density in the Cp π orbitals. Hence, a simple probe for determining the sign of the spin density results after subtracting eq 1b from eq 1a:

$$\Delta\delta^{con} = \Delta\delta_o + 0.6B \quad (2)$$

where $\Delta\delta^{con} = \delta^{con}(C8/9) - \delta^{con}(C10)$ and $\Delta\delta_o = \delta_o(C8/9) - \delta_o(C10)$. In the most simple case both δ_o values are equal so that eq 2 becomes

$$\Delta\delta^{con} = 0.6B \quad (2a)$$

Thus, if $\Delta\delta^{con}$ is positive, the spin density in the Cp π orbitals is also positive and vice versa. As visualized in Figure 8, $\Delta\delta^{con}$ and the spin density in the Cp π orbitals of all compounds is negative except for the neutral and the cationic nickel derivative. While this result was expected theoretically,[2,4] it is gratifying that in the crucial case of vanadocenes the present spin probe unequivocally establishes negative spin.

Other Spin Density Features. A more detailed analysis must take δ_o into account which represents the sum of all nonhyperconjugative contributions to the contact shifts (eq 1). In principle, these contributions must be different for C8/9 and C10 for the following reasons. (i) The spin transfer does not only depend on the angle θ (eq 1 and Figure 3, **F**) but also on ϑ(C8/9) and ϑ(C10) (Figure 4, **G**) which are different (Table 1). Consideration of ϑ leads to a positive $\Delta\delta_o$. (ii) Polarization[25] of the bonds C1/7−C8/9 and C1/7−C10 through spin in the Cp π orbitals either directly (contribution to $\Delta\delta_o$ unknown) or via the bonds C2/6−C1/7 (consecutive polarization which should be small[25]). (iii) σ-Delocalization which transmits positive spin from the metal to all carbon atoms of the ligand thus shifting the signals of C8/9 and C10 to more positive values. In any of the two latter cases C8/9 and C10 should be affected differently.

(23) Switzer, M. E.; Rettig, M. F. *J. Chem. Soc., Chem. Commun.* **1972**, 687.

(24) Kurland, R. J.; McGarvey, B. R. *J. Magn. Reson.* **1970**, *2*, 286.

(25) (a) Adam, F. C.; King, F. W. *J. Chem. Phys.* **1973**, *58*, 2446. (b) Ellinger, Y.; Subra, R.; Levy, B.; Millie, P.; Berthier, G. *J. Chem. Phys.* **1975**, *62*, 10.

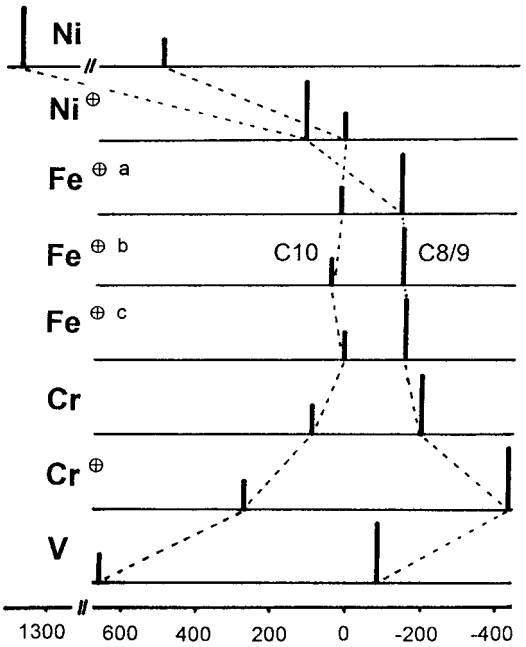

Figure 8. Metal-dependent trends of the Fermi contact shifts of C8/9 and C10 within the series $(Isodicp)_2M$; scale in ppm: (a) *exo,exo*-isomer; (b) *exo,endo*-isomer, *exo*-ligand; (c) *exo,endo*-isomers, *endo*-ligand.

If only hyperconjugation is effective, the contact shifts of both C8/9 and C10 should be positive for the neutral and cationic nickel derivatives and negative for all other compounds. As Figure 8 shows, this is true for the nickel derivatives. By contrast, all other compounds have positive and negative contact shifts for C10 and C8/9, respectively. We ascribe this to σ-delocalization which can be formulated as a σ-contribution $\Delta\delta_{o,\sigma}$ to the overall term $\Delta\delta_o$ in eq 2. Both the nonhyperconjugative term $\Delta\delta_{o,\sigma}$ and the hyperconjugative term B (eq 2) depend on the metal. Thus the spacing of the signals of C8/9 and C10 increases with B. According to Figure 8 the trend is $B(Fe^+) < B(Cr) < B(Cr^+) \sim B(V)$. The second obvious trend is that of the σ-delocalization with $\Delta\delta_{o,\sigma}(Fe^+) \sim \delta_{o,\sigma}(Cr) \sim \Delta\delta_{o,\sigma}(Cr^+) < \Delta\delta_{o,\sigma}(V)$. Here we assume that C8/9 and C10 do not behave very differently. The general message from these trends is that whenever σ-delocalization is important for any type of sandwich compounds (e.g. for vanadocenes) it will vary strongly for different derivatives. In these cases it is not advisable to probe the sign of the spin density by using two different molecules as mentioned in the Introduction.

Further information on the spin distribution in $(Isodicp)_2M$ is contained in the signal separation of the Cp protons H3/5 and H4. It is strikingly larger than for other substituted paramagnetic metallocenes. This is most evident when the two 1,2-dialkylated compounds $(Isodicp)_2M$ and $(1,2\text{-}Me_2C_5H_3)_2M$[26] are compared. For the first series the separation of the signals of H3/5 and H4 at 298 K is 19.1, 65.5, 1.6, and 107.3 ppm for M = Ni, Co, Fe^+, and Cr, respectively; for $(1,2\text{-}Me_2C_5H_3)_2M$ the corresponding sequence is only 0, 25.0, 0, and 26 ppm. The difference must be ascribed to the ligand part of the spin-containing MOs. Throughout the metallocene series the relevant MOs have one modal plane orthogonal to the Cp plane (e_1-type MOs of Cp^-).[18c] For a qualitative understanding extended Hückel calculations were carried out for $(Isodicp)_2Ni^+$ the relevant orbitals of which are shown in Figure 9. The contact shift of H3−5 is proportional to the spin on the neighboring carbon atom, and the spin density can be approximated by the squared carbon $2p_z$ coefficients. Hence spin in MO 55 entails the signal sequence $|\delta^{con}(H3/5)| < |\delta^{con}(H4)|$ while it is inverted for MO 56. The relative energy of both MOs determines the separation of the signals of H3/5 and H4: It increases with the energy gap between both MOs and thus with the perturbation of the Cp ligand through substitution. When passing from $(Isodicp)_2Ni^+$ to $(1,2\text{-}Me_2C_5H_3)_2Ni^+$ the signal separation may also result from changes of the $2p_z$ coefficients at C3−5. Our calculations show that the latter effect is much less important than the energy gap. In the particular case of $(Isodicp)_2Ni^+$ the signal shifts in Table 2 mean that the unpaired electron sits mainly in MO 56 and that only little spin is located at C4. It is worth mentioning that Figure 9 also reflects the hyperconjugtive engagement of the bonds C1/7−C8/9 and C1/7−C10 in the spin delocalization that was already discussed.

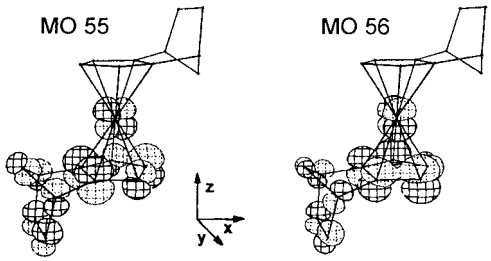

Figure 9. Ligand orbitals of $(Isodicp)_2Ni^+$ that are engaged in spin delocalization. For clarity the contributions to MO 55 and 56 of all hydrogens and the carbons of one ligand have been omitted.

When compounds other than $(Isodicp)_2Ni^+$ are considered the signal sequence of H3/5 and H4 may be inverted. An instructive example is $(Isodicp)_2Cr$ which also has one unpaired electron in an e_1-type set of MOs.[18c] According to Table 2 δ^{con}(H4) is now bigger than δ^{con}(H3/5) which means that an orbital similar to MO 55 dominates the spin distribution. This situation resembles that of the isodicyclopentadienyl radical and confirms the assumption of Faucitano et al.[27] that H4 should be most affected. Comparison of the EPR work[27] and the present NMR results clearly demonstrate that NMR spectroscopy provides far superior information when the radical can be transormed to a metal-bound ligand which carries less spin than the pure radical.

Conclusion

In view of the mechanism that determines the magnetic interaction within stacks of metallocenium tetracyanoethenide and the like the dertermination of the spin sign on π ligands has been studied by NMR spectroscopy. It turned out that this method is most reliable when ^{13}C NMR spectroscopy and the isodicyclopentadienyl (Isodicp) ligand are used.

The necessary neutral and cationic paramagnetic model compounds are available from the reaction of $Isodicp^-$ with metaldihalides. Two crystal structures show that the ligand geometry hardly changes so that standard distances and angles can be used for the calculation of the relevant contact shifts from the experimental ^{13}C and ^1H NMR data. The key feature of $(Isodicp)_2M$ with respect to spin probing are two different types of carbon atoms which are separated from the spin-containing ligand π orbitals by two bonds (β carbons). Owing to hyperconjugation the β carbon signals experience different contact shifts which allow to unequivocally determine the spin sign.

(26) Doll, K.-H.; Köhler, F. H., unpublished results.

(27) Faucitano, A.; Buttafava, A.; Faucitano Martinotti, F.; Cesca, S.; Fantechi, R. *J. Phys. Chem.* **1977**, *81*, 354.

Generally, the most important source of error is σ spin delocalization. This error can be minimized by studying a unique model compound rather than by comparing two different ones. In addition, the NMR data allow to establish molecular spin maps and to sort out the MOs which predominately accommodate the unpaired electrons.

Exprimental Section

The syntheses and the characterization of all compounds were carried out under dry and oxygen-free dinitrogen or argon. The solvents were dried and freed from oxygen by using standard methods. Unless stated otherwise the reagents were purchased; $FeCl_2(THF)_{1.5}$,[28a] $NiBr_2(THF)_{1.5}$,[28b] $CrCl_2(THF)$,[28c] $AgPF_6(MeCN)_3$,[28d] $[Cp_2Fe]^+[PF_6]$,[28e] and **4a**[11b,28f] were prepared following the literature. The melting and decomposition points were determined in sealed capillaries, and the elemental analyses were carried out by the Inorganic Microanalytical Laboratory at Garching.

Tricyclo[5.2.1.0^{2,6}]deca-2,4-dien-6-yllithium (Isodicyclopentadienyllithium) (2). In a modified literature procedure,[13] 163 mL (1.2 mol) of dicyclopentadiene was added to a black suspension of 0.73 g of Pd/C (10% Pd on carbon black) in 330 mL of ethanol. The reaction vessel was flushed twice with H_2 before the mixture was stirred vigorously with continuous access of H_2. After the H_2 uptake was finished (37.8 L versus theoretical 27 L) the reaction mixture was poured into 400 mL of water, extracted with three portions of 800 mL of Et_2O, and the organic phase was passed over Na_2SO_4. Stripping of the solvent and drying in vacuo gave 150.3 g (93% yield) of *endo*-tricyclo[5.2.1.0^{2,6}]dec-3-ene.

This product was further converted by modifying previous work.[13] A solution of 235.9 g (1.76 mol) of *endo*-tricyclo[5.2.1.0^{26}]dec-3-ene and 33.56 g (0.24 mol) of KH_2PO_4 in 850 mL of dioxane containing 10% of H_2O was heated to 90 °C. To this solution was added 100.95 g (0.91 mol) of SeO_2, and the mixture was stirred and refluxed for 3 h during which time it became deep red. The mixture was allowed to cool to ambient temperature and was then filtered, and 3 L of Et_2O was added to the liquid. Washing with four 1-L portions of a 10% aqueous solution of Na_2CO_3, separating the organic layer, drying with $MgSO_4$, stripping the solvent, and distillation under reduced pressure gave 99.5 g (0.74 mol) of the educt (bp 68 °C/1.3 $\times$ 10^{-3} bar) and 83.9 g (55% yield relative to consumed educt) of 5*S*-hydroxy-*endo*-tricyclo[5.2.1.0^{2,6}]dec-3-ene (bp 22 °C/1.3 $\times$ 10^{-3} bar).

A 74.8-g amount (0.5 mol) of the alcohol of the previous step was warmed to 60 °C in a heatable dropping funnel. Subsequently it was allowed to pass dropwise through a quartz tube that was filled with Al_2O_3 (Alcoa Chemicals S-400, 3/16", fitting height 23 cm) and heated to 320 °C. The reaction products were collected in a trap which was placed at the outlet of the quartz tube and kept at −78 °C and 0.15 bar. Workup as described for the previous step and distillation under reduced pressure gave 33.88 g of **1** (bp 65 °C/1.6 $\times$ 10^{-2} bar) and 9.73 g of the educt (yield 50.5% relative to consumed educt).

For the deprotonation 21.43 g (0.16 mol) of **1** was dissolved in 100 mL of hexane, cooled to −78 °C and reacted with 70 mL of a 2.5 molar solution of *n*-BuLi in hexane (0.175 mol) which was added dropwise with stirring. The reaction mixture was allowed to warm to room temperature, and the white solid was collected on a frit and washed three times with hexane. Drying in vacuo gave 19.49 g (yield 88.2%) of **2**. Data for **2**: ^{1}H NMR (DMSO-d_6, 298 K) δ 4.98 (m, 1H) H4; 4.93 (m, 2H) H3/5; 2.93 (s, 2H) H1/7; 1.58 (m, 2H) H8/9-*anti*; 1.42 (m, 1H) H10-*syn*; 1.32 (m, 1H) H10-*anti*; 0.70 (m, 2H) H8/9-*syn*; ^{13}C NMR (DMSO-d_6, 298 K) δ 127.3, C2/6; 102.3, C3/5; 93.0, C4; 51.1, C10; 41.0, C1/7; 31.0, C8/9. The signal shifts deviate significantly from literature reports,[16f] because a different solvent was used.

***exo,exo*- and *exo,endo*-Bis(tricyclo[5.2.1.0^{2,6}]deca-2,4-dien-6-yl)-iron (3a and 3b).** In a modified literature procedure[15] 3.14 g (13.4 mmol) of $FeCl_2(THF)_{1.5}$ was suspended in 50 mL of THF, the mixture was warmed to 40 °C, and a solution of 3.43 g (24.8 mmol) of **2** in 40 mL of THF was added dropwise. The mixture was stirred for 1 h at 40 °C and allowed to cool to room temperature, and the solvent was removed in vacuo. To the residue was added 20 mL of diluted HCl and 100 mL of Et_2O, the mixture was stirred, and the phases were separated. The green aqueous phase was washed twice with 50-mL portions of Et_2O, and the combined orange organic phases were washed with 50 mL of a 10% solution of $NaHCO_3$ in water. Drying of the organic phase over $MgSO_4$ and removing the solvent in vacuo gave 2.50 g of a crude product that contained **3a** and **3b**. When a saturated solution of this material in acetone at 50 °C was allowed to cool to room-temperature gold-brown cystals of pure (NMR) **3a** separated very slowly. This procedure was repeated until no traces of **3b** could be detected by NMR spectroscopy in the crystal fraction of **3a**.The total yield of **3a** was 840 mg (21.1%). **3a** could be further separated from **3b** by fractional crystallization until **3b** was only slightly contaminated with **3a**. This material was used for NMR studies. Data for **3a**: ^{1}H NMR ($CDCl_3$, 298K) δ 3.93 (m, 2H) H4; 3.70 (m, 4H) H3/5; 2.84 (m, 4H) H1/7; 2.30 (m, 2H) H10-*syn*; 1.69 (m, 4H) H8/9-anti; 1.36 (m, 2H) H10-anti; 0.96 (m, 4H) H8/9-*syn*; ^{13}C NMR ($CDCl_3$, 298K) δ 98.4, C2/6; 67.5, C4; 59.4, C3/5; 47.7, C10; 37.5, C1/7; 28.3, C8/9. Anal. Calcd for $C_{20}H_{22}Fe$: C, 75.49; H, 6.97. Found: C, 75.18; H, 7.11. Data for **3b**: ^{1}H NMR (C_6D_6, 298 K), *exo*- and *endo*-coordinated ligand, respectively, δ 3.93 and 3.75 (m, ^{1}H each) H4; 3.90 and 3.74 (m, 2H each) H3/5; 2.80 and 2.70 (m, 2H each) H1/7; 2.33 and 1.89 (m, 1H each) H10-*syn*; 1.57 and 2.10 (m, 2H each) H8/9-*anti*; 1.24 and 1.66 (m, 1H each) H10-*anti*; 1.00 and 1.97 (m, 2H each) H8/9-*syn*; ^{13}C NMR (C_6D_6, 298K), *exo*- and *endo*-coordinated ligand, respectively, δ 97.5 and 106.3, C2/6; 59.8 and 55.7, C4; 55.3 and 52.9, C3/5; 43.8 and 52.3, C10; 36.2 and 36.3, C1/7; 28.4 and 31.4, C8/9.

***exo,exo*- and *exo,endo*-Bis(tricyclo[5.2.1.0^{2,6}]deca-2,4-dien-6-yl)-iron Hexafluorophosphate (3a$^+$ PF$_6^-$ and 3b$^+$PF$_6^-$).** A 1.30-g amount (4.1 mmol) of **3a** was dissolved in 50 mL of THF, the solution was cooled to −78 °C, and a solution of 1.59 g (4.23 mmol) of $AgPF_6(MeCN)_3$ in 80 mL of THF was slowly added from a dropping funnel. This was accompanied by a color change from orange to dark green. The mixture was brought to room temperature and passed through a frit which was partly filled with Na_2SO_4. THF was stripped from the solution, the remainder was dissolved in a few mL of acetone, and hexane was slowly added until a green precipitate formed. The precipitate was allowed to settle, the liquid was removed via cannula, and the solid was washed with hexane. Drying in vacuo gave 1.66 g of a product which was further purified by recrystallization from acetone/hexane to yield 950 mg (50%) of dark green **3a**$^+$PF$_6^-$. When heated **3a**$^+$PF$_6^-$ decomposed above 160 °C. Anal. Calcd for $C_{20}H_{22}F_6FeP$: C, 51.86; H, 4.79; Fe, 12.06. Found: C, 49.23; H, 4.48; Fe, 12.00.

Similarly, a sample that contained about 83% of **3b** and 17% of **3a** was oxidized to **3b**$^+$PF$_6^-$ (in the presence of some **3a**$^+$PF$_6^-$).

***exo,exo*-Bis(tricyclo[5.2.1.0^{2,6}]deca-2,4-dien-6-yl)chromium (5a).** Following the general procedure for the preparation of chromocenes[28c] 2.01 g (8.5 mmol) of $CrCl_2(THF)$ was dissolved in 40 mL of THF, the solution was heated to 40 °C, and a solution of 2.35 g (17 mmol) of **2** dissolved in 35 mL of THF was added dropwise. The mixture which changed color from turquoise to brown was stirred for 30 min at 40 °C and cooled to room temperature. After the solvent was stripped, the residue was extracted with hexane until the hexane fraction was colorless, and the solution was reduced to about 30 mL. Cooling to −28 °C gave 1.33 g (4.9,8% yield) of **5a** as red crystals, mp 146−148 °C. MS (EI, 70 eV; *m*/*z* (%)): 312 (2), M$^+$ − 2H; 264 (2), M$^+$ − Cr); 132 (33), isodicyclopentadiene$^+$); 104 (100), C_8H_8). Anal. Calcd for $C_{20}H_{22}Cr$: C, 76.41; H, 7.05. Found: C, 76.77; H, 7.34.

***exo,exo*-Bis(tricyclo[5.2.1.0^{2,6}]deca-2,4-dien-6-yl)chromium Hexafluorophosphate (5a$^+$PF$_6^-$).** A solution of 2.46 g (7.3 mmol) of $Cp_2Fe^+PF_6^-$ in 150 mL of acetone was added dropwise to 2.33 g (7.4 mmol) of solid **5a** while the mixture was stirred. Subsequently it was filtered, the solution was reduced to ca. 50 mL, and hexane was added whereupon a greenish yellow solid precipitated. Repeated crystallization from acetone/hexane gave 1.20 g (36% yield) of **5a**$^+$PF$_6^-$ as a

(28) (a) Kern, R. J. *J. Inorg. Nucl. Chem* **1962**, *24*, 1105. (b) Müller, R. Thesis, Technische Universität München, 1986. (c) Köhler, F. H. *Organometallic Syntheses*; King, R. B., Eisch, J. J., Eds.; Elsevier: Amsterdam, 1988; Vol. 4, p 52. (d) Padma, D. K. *Synth. React. Inorg. Met.-Org. Chem.* **1988**, *18*, 401. (e) Schumann, H. *J. Organomet. Chem.* **1986**, *304*, 341. (f) Köhler, F. H. *Organometallic Syntheses*; King, R. B., Eisch, J. J., Eds.; Elsevier: Amsterdam, 1988; Vol. 4, p 15.

microcrystalline powder; mp 212 °C. NMR-spectroscopically pure $\mathbf{5a}^+PF_6^-$ proved to be partly converted to chromium carbides when subjected repeatedly to elemental analysis. Anal. Calcd for $C_{20}H_{22}CrF_6P$: C, 52.30; H, 4.83; Cr, 11.29. Found: C, 51.03; H, 4.80; Cr, 10.21.

***exo,exo-*, *exo,endo-*, and *endo,endo*-Bis(tricyclo[5.2.1.0^{2,6}]deca-2,4-dien-6-yl)cobalt Hexafluorophosphate ($\mathbf{6a}^+PF_6^-$, $\mathbf{6b}^+PF_6^-$, and $\mathbf{6c}^+PF_6^-$).** A sample of $CoCl_2$ (2.44 g, 18.8 mmol) was suspended and stirred for 12 h in a mixture of 150 mL of THF and 50 mL of Et_3N. The resulting dark blue solution was warmed to 40 °C, 5.29 g (38.3 mmol) of solid **2** was added, and the brown mixture was stirred for 1 h. Subsequently, 3.70 g (32.6 mmol) of $FeCl_3$ dissolved in 50 mL of diluted hydrochloric acid was added to the stirred solution by using a pipet, the liquids were removed in vacuo, the solid was dissolved in water, and the solution was purified by extracting three times with Et_2O and by filtering. Addition of a 4-fold molar excess of 12.48 g (76.6 mmol) of $NH_4^+PF_6^-$ gave a yellow solid which was recrystallized from acetone to yield 5.62 g (64.4%) of a microcrystalline mixture of $\mathbf{5a}^+PF_6^-$, $\mathbf{5b}^+PF_6^-$, and $\mathbf{5c}^+PF_6^-$; the ratio was 2.5/4.2/1, respectively, as determined by ^{1}H NMR spectroscopy. Anal. Calcd for $C_{20}H_{22}CoF_6P$: C, 51.52; H, 4.75. Found: C, 51.26; H 4.87. Data for $\mathbf{5a}^+$: ^{1}H NMR (acetone-d_6, 298K) δ 5.59 (broad, 2H) H4; 5.46 (m, 4H) H3/5; 3.25 (m, 4H) H1/7; 2.33 (m, 2H, ^2J(HH) = 10.5 Hz) H10-*syn*; 1.94 (m, 4H, ^2J(HH) = 8.9 Hz) H8/9-*anti*; 1.75 (m, 2H, ^2J(HH) = 9.8 Hz) H10-*anti*; 1.13 (m, 4H, ^2J(HH) = 8.2 Hz) H8/9-*syn*; ^{13}C NMR (acetone-d_6, 298K) δ 115.6 (d, ^2J(CH) = 8.8 Hz) C2/6; 82.9 (dt, ^1J(CH) = 181.2 Hz, ^2J(CH) = 6.1 Hz) C4; 74.8 (dt, ^1J(CH) = 190.0 Hz, ^2J(CH) = 6.1 Hz) C3/5; 50.3 (tt, ^1J(CH) = 136.1 Hz, ^2J(CH) = 7.7 Hz) C10; 37.7 (dm, ^1J(CH) = 153.4 Hz, ^2J(CH) = 7.7 Hz) C1/7; 26.8 (t, ^1J(CH) = 134.4 Hz) C8/9. Data for $\mathbf{5b}^+$: ^{1}H NMR (acetone-d_6, 298 K) *exo*- and *endo*-coordinated ligand, respectively, δ 5.61 and 5.50 (m, 1H each) H4; 5.49 and 5.53 (m, 2H each) H3/5; 3.18 and 3.37 (m, 2H each) H1/7; 2.07 and 2.11 (m, 1H each, ^2J(H,H) = 10.5 and 10.0 Hz) H10-*syn*; 1.92 and 2.34 (m, 2H each, ^2J(H,H) = 8.9 Hz both) H8/9-*anti*; 1.75 and 1.95 (m, 1H each, ^2J(H,H) = 9.8 and 9.6 Hz) H10-*anti*; 1.11 and 1.89 (m, 2H each, ^2J(H,H) = 8.3 and 8.2 Hz) H8/9-*syn*. ^{13}C NMR (acetone-d_6, 298 K) *exo*- and *endo*-coordinated ligand, respectively, δ 115.4 and 126.2, C2/6; 82.5 and 77.1 (d, ^1J(CH) = 185 and 190.0 Hz) C4; 74.4 and 76.2 (d, ^1J(CH) = 190.0 and 185.5 Hz) C3/5; 49.7 and 57.7 (t, ^1J(CH) = 136.9 and 136.1 Hz), C10; 38.0 and 38.6 (d, ^1J(CH) = 153.6 and 149.8 Hz) C1/7; 26.7 and 32.1 (t, ^1J(CH) = 134.4 and 127.8 Hz) C8/9. Data for $\mathbf{5c}^+$: ^{13}C{^{1}H} NMR (acetone-d_6, 298 K) δ 125.6, C2/6; 76.6, C4; 76.7, C3/5; 57.5, C10; 38.8, C1/7; 32.4, C8/9.

***exo, exo*-Bis(tricyclo[5.2.1.0^{2,6}]deca-2,4-dien-6-yl)nickel Hexafluorophosphate ($\mathbf{7a}^+PF_6^-$).** A sample of 1.19 g (3.7 mmol) of **7a**[11b] in 20 mL of acetone was oxidized by adding a solution of 1.20 g (3.6 mmol) of $Cp_2Fe^+PF_6^-$ in 90 mL of acetone and worked up as described for $\mathbf{5a}^+$. Washing of the crude product with hexane gave 1.42 g (yield 84.2%) of red-brown microcrystalline $\mathbf{7a}^+PF_6^-$; mp 224−227 °C (dec). Anal. Calcd for $C_{20}H_{22}F_6NiP$: C, 51.54; H, 4.76. Found: C, 51.16; H, 4.80.

Measurements and Calculations. A Varian MAT 311 A spectrometer was used in the elctron impact mode for recording the mass spectra. The NMR spectra were obtained from Bruker MSL 300, Bruker AMX 600, and JEOL JNM GX 270 spectrometers by using tubes with ground glass and stoppers; solenoid tubes[29] were used for ^{13}C NMR. A Pt resistance thermometer (Merz MN 100) ensured the temperature calibration. Routinely (6−12) × 10^{-2} molar solutions of the compounds were used, the number of accumulations was 10^2−10^3 and 10^4−10^5 (depending on the signal width) for ^{1}H and ^{13}C NMR spectra, respectively, and the repetition time was 200 ms. All signals were measured relative to solvent peaks. The signal shifts of the solvents[30] and those of **3a**, **3b** $\mathbf{6a}^+PF_6^-$, and $\mathbf{6b}^+PF_6^-$ served as standards for the calculation of TMS-based and paramagnetic signal shifts, respectively; the calculation of the dipolar and contact shifts is given in the Supporting Information. The EPR spectra were obtained from a JEOL JES RE 2X spectrometer.

Table 3. Crystal Structure Data

compound	$\mathbf{3a}^+PF_6^-$	$\mathbf{5a}^+PF_6^-$
empirical formula	$C_{20}H_{22}F_6FeP$	$C_{20}H_{22}CrF_6P$
fw	463.19 g mol^{-1}	459.37 g mol^{-1}
$a = b$	9.708(1) Å	9.736(1) Å
c	16.566(2) Å	16.750(1) Å
γ	120°	120°
V	1352.1(3) Å^3	1375.0(2) Å^3
Z	3	3
space group	$P3_121$ (No. 152)	$P3_121$ (No. 152)
T	199(2) K	205(2) K
λ	0.710 73 Å	0.710 73 Å
ρ_{calcd}	1.707 g cm^{-3}	1.664 g cm^{-3}
abs coeff	0.988 mm^{-1}	0.773 mm^{-1}
R [$F_o > 4\sigma(F_o)$]	$R_1{}^a = 0.0439$	$R_1 = 0.0548$
	$wR_2{}^b = 0.1239$	$wR_2 = 0.1505$

^{a} $R_1 = \sum||F_o| - |F_c||/\sum|F_o|$. ^{b} $wR_2 = [\sum[w(F_o^2 - F_c^2)^2]/\sum[w(F_o^2)^2]]^{1/2}$, $w = 1/[\sigma^2(F_o^2) + (0.1043P)^2 + 2.3991P]$, where $P = (F_o^2 + 2F_c^2)/3'$.

The X-ray crystal structure determinations were carried out with crystals which were grown at room temperature by diffusion of hexane into a solution of $\mathbf{3a}^+PF_6^-$ in THF and by cooling a solution of $\mathbf{5a}^+PF_6$ in CH_3NO_2. The crystals were sealed in a thin-walled glass capillary under argon for use in the diffraction experiment. All investigations were performed on a Nonius CAD4 four-circle diffractometer with Mo Kα radiation (graphite monochromator) at low temperature of 205 K ($\mathbf{3a}^+PF_6^-$) and 199 K ($\mathbf{5a}^+PF_6^-$). Accurate cell dimensions were determined from the setting angles of 100 centered reflections. Integrated intensities were collected by the ω scan technique. During data collection the intensity of three standard reflections, monitored every 200 reflections indicated stable measuring conditions. The structure was solved by direct methods and refined on F^2 with the program package SHELXTL. Hydrogen atoms were placed in calculated positions. Experimental crystallographic data are summarized in Table 3, selected bond lengths and angles are given in Table 1 and in the Supporting Information, and perspective views are presented in Figure 4. Further data and details are available upon request at the Fachinformationzentrum Karlsruhe, D-76344 Eggenstein-Leopoldshafen, Germany, by quoting the numbers CSD-406424 ($\mathbf{3a}^+PF_6^-$) and CSD-406425 ($\mathbf{5a}^+PF_6^-$).

The MO calculations were performed with the program CACAO,[31] version 4.0. Symmetrized mean values of the crystal structure data were used for the Isodicp ligand. For the 1,2-$M_2C_5H_3$ ligand the same values were used and the bicyclic substituent was replaced by two sandard methyl groups. An estimated value of 1.86 Å was used for the Ni−Cp distance.

Acknowledgment. We are indebted to Dr. R. Feher for recording the EPR spectra and to J. Riede for collecting the X-ray data. This work was supported by the Deutsche Forschungsgemeinschaft and the Fonds der Chemischen Industrie.

Supporting Information Available: HMQC spectra of **3b**, $\mathbf{6a}^+PF_6^-$, and $\mathbf{6b}^+PF_6^-$; ^{1}H spectra of **4a**, **5a**, $\mathbf{5a}^+PF_6^-$, **7a**, and $\mathbf{7a}^+PF_6^-$; and ^{13}C NMR spectra of $\mathbf{3a}^+PF_6^-$, $\mathbf{3b}^+PF_6^-$, and **4a**, and calculation of the dipolar signal shifts as well as X-ray crystallographic files, in CIF format, for compounds $\mathbf{3a}^+PF_6^-$ and $\mathbf{5a}^+PF_6^-$ are available free of charge via the Internet at http://pubs.cas.org.

IC9812407

(29) Köhler, F. H.; Metz, B.; Strauss, W. *Inorg. Chem.* **1995**, *34*, 4402.
(30) Kalinowski, H.-O.; Berger, S.; Braun, S. *^{13}C-NMR-Spectroskopie*; Georg Thieme Verlag: Stuttgart, 1989; p 74.
(31) Mealli, C.; Prosperio, D. M. *J. Chem. Educ.* **1990**, *67*, 399.